Academic Science Journal

The Effect of Double Doping with Copper and Tin on the Structural and Optical Properties of Nickel Oxide Nanoparticles Prepared by Sol-Gel Method

S. A. Mohammed, J. Al-Zanganawee* and O. A. Muwaffaq

Department of Physics – College of Science – University of Diyala

Alzanganawee@uodiyala.edu.iq

Received: 26 September 2022 **Accepted: 13 November 2022**

DOI: https://doi.org/10.24237/ASJ.01.04.687C

Abstract

This work used the Sol-Gel method to prepare NiO nanoparticles that were both undoped and doped by Copper and Tin. According to the XRD data, every sample is polycrystalline. Scherrer's equation was used to calculate the crystallite size of the samples, and it was found that the crystallite size (7.2841, 4.97262, 4.97262, 10.07331, 5.63056 and 5.39887 nm) for undoped (NiO), and doped (d_1, d_2, d_3, d_4 and d_5) respectively, were d is the doping ratio. According to an FTIR spectrum of NiO NPs, showed absorption peaks at the two regions (1566 and 1332 cm^{-1}) Due to the bonds (H-O-H, C-H) respectively, FESEM image for undoped and doped of NiO nanoparticle, shows that the structure with a spherical shape. The spectrum also showed absorption peaks in the region (400-500 cm^{-1}) which is due to the stretching vibration of the (Ni-O) band. The percentage filled by grafting atoms (Cu + Sn). Optical measurements show that the transmittance increases as wavelength increases. The photoluminescence measurement shows that the sample before doping has a peak value of (489.3 nm), and the double-grafted grains record peak values at (367.2, 368.1, 681.1, 582.2, 772.7, 438.6 nm) for pure NiO, d_1, d_2, d_3, d_4 and d_5) respectively, and the value of the energy gap was (3.377, 3.369, 1.821, 2.129, 1.704 and 2.827 eV) for (pure NiO, d_1, d_2, d_3, d_4 and d_5) respectively.

Keywords: Nickel oxide, Sol- Gel, FESEM, Optical Measurements and Photoluminescence.

Academic Science Journal

تأثير التطعيم بالنحاس والقصدير على الخواص التركيبية والبصرية لجسيمات اوكسيد النيكل NiO المحضرة بطريقة الـ(SoL-gel)

سندس احمد محمد، جاسم محمد منصور وعمر احمد موفق

قسم الفيزياء – كلية العلوم – جامعة ديالى

الخلاصة

استخدم هذا العمل طريقة Sol-Gel لتحضير جزيئات NiO النانوية غير المطعم بالنحاس والقصدير. وفقًا لنتائج XRD ، فان العينات متعددة التبلور بتركيب مكعب وبطور سائد (200). تم استخدام معادلة شيرير لحساب الحجم البلوري للعينات، ووجد أن الحجم البلوري لكل من أوكسيد النيكل غير المطعم والمطعم بالنحاس والقصدير (7.2841، 4.97262، 4.97262، 10.07331، 5.63056 و 5.39887 نانومتر) حسب نسب التطعيم المشار لها بالرموز (d_1، d_2 ، d_3 ، d_4 و d_5) على التوالي. وفقًا لطيف FTIR الخاص بـجسيمات NiO النانوية غير المطعم والمطعم بالنحاس والقصدير، أظهرت قمم الامتصاص في المنطقتين (1566 and 1332 cm^{-1}) التي تعود الى الاواصر (H-O-H, C-H)على التوالي، تُظهر صورة FESEM لجسيمات NiO النانوية غير المطعمة والمطعمة، يمتلك تركيب كروي الشكل كما وقد ظهرت قمم FTIR الامتصاص في المنطقتين في المنطقة (400 - 500 cm^{-1}) الناتجة عن اهتزازات الاصرة (Ni-O). تظهر القياسات البصرية أن النفاذية تزداد مع زيادة الطول الموجي. يُبين قياس الضيائية أن العينة قبل التطعيم لها قيمة ذروة تبلغ (489.3 nm) ، اما بعد التطعيم فقد سجلت القيم التالية (367.2, 368.1, 681.1, 582.2, 772.7, 438.6 nm) على التوالي وبلغت قيم فجوة الطاقة (3.377, 3.369, 1.821, 2.129, 1.704 and 2.827 eV) لـ (NiO، d1، d2، d3، d4، d5) على التوالي.

الكلمات المفتاحية: اوكسيد النيكل، صول جيل، FESEM، القياسات البصرية والتألق الضوئي.

Introduction

NiO, one of several nanostructured metal oxides, has caught the interest of scientists and researchers due to its fundamental scientific applications. A promising contender for use in optical amplifiers, tunable lasers, magnetic materials, catalytic materials, sensitive materials for chemoresistive or optical gas sensors, and other applications, nickel (II) oxide is one of the few transition metal oxides with a predisposition to be p-type [1]. The creation of the NiO NPs manufacturing process has required a lot of effort. Although it is still in its early stages, research synthesizing of nanostructured nickel oxide has primarily concentrated powder, solution, and thin films [3-5]. Sol-gel [3], microwave plasma [4], co-precipitation, and hydrothermal [2] are

just a few of the processes that can be used to prepare NiO nanoparticles. The aim of this research is to use the sol-gel method to prepare NiO nanoparticles and investigate how the doping copper and tin effect on the structural, morphological and optical properties of these samples.

Experimental Details

1. Dissolving each of the queous nickel nitrate ($Ni\ (NO_3)_2.6H_2O$), aqueous copper nitrate ($Cu\ (NO_3)_2.3H_2O$) and aqueous tin chlorides ($SnCl_2.2H_2O$) in (200 ml) of distilled water at a concentration (0.3M) by a magnetic stirrer for (30 min) at room temperature, and Table (1) shows the weights used to obtain the required percentages.

2. Dissolving citric acid $C_6H_8O_7.H_2O$ in (100 ml) and at a concentration (0.2M) of distilled water at room temperature, as shown in Table (1).

3. Adding the citric solution (4.2028g) in the form of drops to the mixture of nickel nitrate, copper nitrate and tin chloride solution by a magnetic stirrer for 30 min at room temperature to ensure complete homogeneity of the solutions.

4. Modifying the pH function using the pH scale to reach approximately (5.5) by adding ammonia hydroxide solution in the form of drops.

5. Putt the resulting solution on a magnetic stirrer, raise the temperature and fix it to (75°C). After a while, the gases begin to rise and the reaction is left for a while continuing to stir the solution until the gel form (gel) is formed.

6. After the gel form is formed, it is cooled and then dried in a thermal oven at (100 ^{o}C) for (10 h), then we get the compound in the form of a powder.

7. Put the resulting powder in a bowl of high-temperature resistant porcelain and then put it in an oven for the purpose of calcination at (525 $^{\circ}$C) for a period of (3 h), and then grind it with a ceramic mortar well until the powder is homogeneous and we get rid of the lumps that occurred during the calcination process.

Academic Science Journal

Table 1: Represents the weights and molarity used to prepare the nickel oxide nanoparticles.

Sample	Dope ratio %	Ratio of Nickel nitrate %	Ratio of Cupric Nitrate %	Ratio of Tin(II) chloride %	Mass of Nickel nitrate g	Mass of Cupric Nitrate g	Mass of Tin(II) chloride g	Mass of Citric Acid g
NiO-undoped	0	100	0	0	15.70266	0	0	4.2028
d_1	10+0	90	10	0	15.70266	1.4496	0	4.2028
d_2	7.5+2.5	90	7.5	2.5	15.70266	1.0872	0.33847	4.2028
d_3	5+5	90	5	5	15.70266	0.7248	0.67695	4.2028
d_4	2.5+7.5	90	2.5	7.5	15.70266	0.3624	1.015425	4.2028
d_5	0+10	90	0	10	15.70266	0	1.35390	4.2028

Results and Discussions

Results of XRD

The results of X-ray diffraction (XRD) examination of prepared undoped NiO nanoparticles and doped with copper (Cu) and tin (Sn) showed that they are polycrystalline with cubic type structure and preferred orientation was (200). The X-ray diffraction patterns of undoped and co-doped NiO nanoparticles are shown in figure (1). These patterns were analyzed to find the locations of the unit peaks that indicate the extent of crystallization of the prepared nanoparticles. For all undoped and co-doping NiO nanoparticles only five peaks at ($2\theta \sim 37.3^{o}$, 43.3^{o}, 63^{o}, 75.4^{o} and 79.4^{o}) which correspond to the crystal levels (111), (200), (220), (311) and (222) respectively, as a dominant and preferred growth orientation (200) is observed for these nanoparticles, and these results are largely in agreement with the standard card (ICDD No. 047-1049), the other peaks shown in figure (d_1,d_2, d_3, d_4 and d_5) are due to the formation of (Ni and SnO_2), which are designated in the figure by the symbols (* and ♦) respectively. Copper (Cu^{2+} ions= 0.73 Å) and tin (Sn^{4+} ions= 0.69 Å) compared to nickel ion (Ni^{2+} ions= 0.69 Å) leads to an increase in the intensity of the peaks of the XRD pattern and a decrease in the width of the FWHM curves. Increasing the ratios of co-doping compared with the ungrafted NiO granules, and the reason for the improvement of the crystal structure with the increase in the ratios of co-

doping may be due to the compensation of the oxygen spaces by means of copper ions and tin ions [7], or it may be substitutional for ions Nickel [8], which caused an increase in the size of crystals and a decrease in both the intensity of dislocations and internal strain, and previous studies recorded an improvement in the crystal structure upon binary grafting of nickel oxide grains (NiO) [9].

The occupancy of copper ions and tin ions at inter-sites in the crystal lattice of the nickel oxide crystal, which results in a slight difference, is most likely the cause of the difference in peak intensity and full width at half maximum (FWHM) between the different doping ratios shown in Figure1[10]. In general, the results of the (XRD) examination showed that the crystal structure of the prepared nanoparticles was clearly affected by the two grafting processes while preserving the crystal structure, and that creeping in small percentages in the diffraction peaks towards the increase or decrease in the diffraction angles confirms the presence of both copper and tin atoms in the composition of the nickel oxide nanoparticles. (NiO), and we note from the results that the double grafting improves the structural properties and this also supports the presence of both grafting elements (Cu + Sn) in the synthesis of nickel oxide (NiO) nanoparticles.

The distance between the crystalline levels of the prepared grains was calculated based on Bragg's law of diffraction for the ungrafted and grafted grains, and it was found that it is in Ignificant agreement with the International Standard Card (ICDD) No. (047-1049) for the nickel oxide nanoparticles. In this research, the dominant and preferred direction of growth (200) was adopted to find out the extent of the change in the properties of NiO granules when they were double-grafted with copper and tin. The grafted and double grafted with copper and tin, and confirms that the whole process of double grafting affects the crystal structure of the prepared NiO and this is consistent with what the researchers found [11].

$n \lambda = 2 d_{hkl} \sin \theta$ ..... (1)

where, d_{hkl}: The distance between interplanar spacing, θ_B: Brack angle,

λ: (wavelength, n: an integer called the order of reflection,

Academic Science Journal

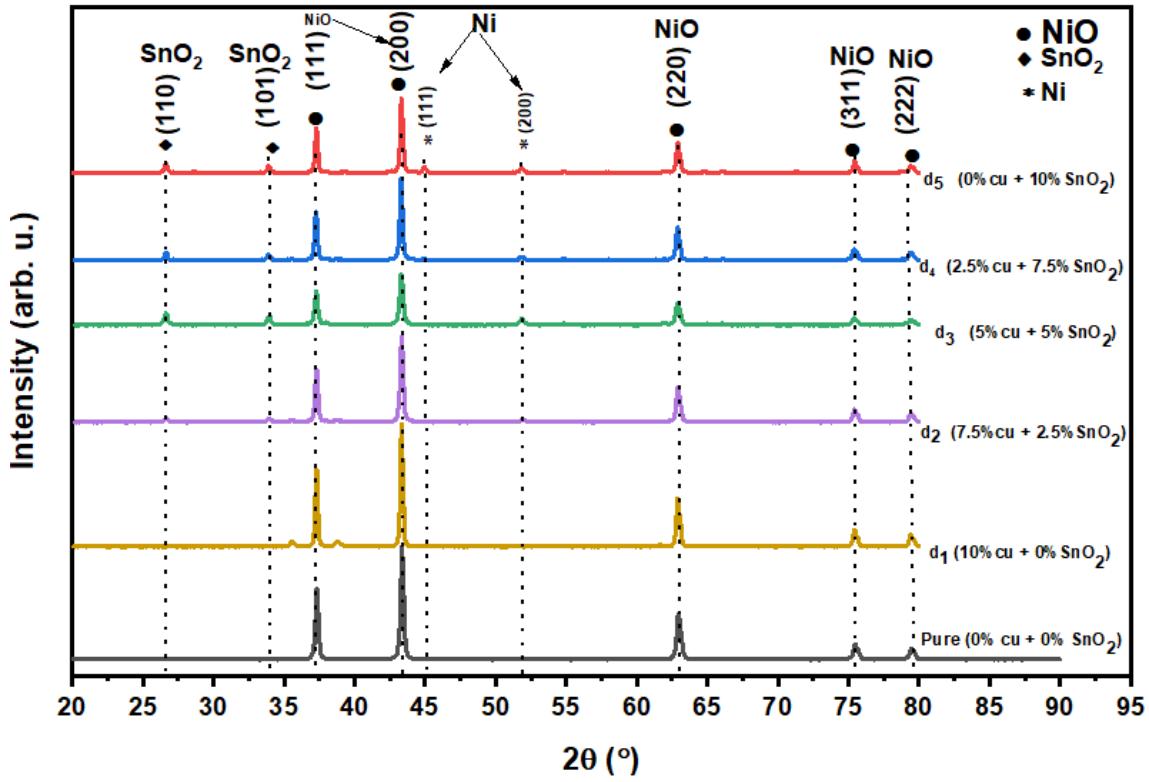

Figure 1: X-ray diffraction patterns of undoped and doped NiO nanoparticles

The size of the crystals (D_{hkl}) was calculated for all the preparations nanoparticles using the relationship (Scherrer's Formula). The results showed that the larger the doping percentage, the higher the crystal size with it, returning to decrease at (d_3) and then increase. (D_{200}) for pure nickel oxide grains are (37.1 nm), and with the increase in the doping percentage, its value begins to increase until it reaches (44.8 nm) for (d_1), which represents the largest value for the crystal size of NiO NPs doping with a ratio of (10% cu + 0 Sn). That is why the aforementioned rise in crystal size is explained by the increase in grain crystallization caused by grafting by Cu^{+2}, which in turn causes an increase in crystal size and a reduction in the width curve of the middle of the big peak [14]. To reach (31.5 nm) for (d_3), which represents the lowest value and then goes back to increase. The value of the crystal size of grains grafted with (10%) of copper is greater than the value of the crystal size of grains of ungrafted nickel oxide, and the reason may be, as mentioned previously, to the occupation of oxygen voids in the synthesis of nickel

oxide by ions doping (copper ion and tin ion) which leads to an increase in crystallization of the grafted grains compared to the undoped NiO NPs [7].

The relationship between the size of the crystals and the width of the (FWHM) of the preferred growth direction (200) for the NiO NPs (undoping and co-dopingin different ratios) is shown in Figure 3; it is also noted that the values of (D) and (FWHM) changed for the direction preferred growth (200) for the different double and different ratios of nickel oxide nanoparticles, as shown in table (2).

$D_{av} = K\lambda / \beta \cos\Theta_B$ ..... (2)

Where, K constant = (0.9), λ: the wavelength of the X-rays falling on the target. β: Full Width at Half Maximum (FWHM) measured in radial units. Table3 shows some of the compositional parameters obtained from X-ray diffraction results

Table 2: Diffraction angles, Miller's coefficients, (FWHM) and interlayer distances and of the as-prepared nanoparticles.

Sample Code	2θ (°)	(hkl)	d_{hkl} (Å)	FWHM (°)
NiO- undoped	43.33**0**	(200)	2.0865	0.2308
d_1	43.33**7**	(200)	2.0862	0.1907
d_2	43.341	(200)	2.0860	0.2135
d_3	43.314	(200)	2.087**3**	0.2714
d_4	43.302	(200)	2.087**8**	0.2029
d_5	43.329	(200)	2.086**6**	0.1987

Table 3: Some parameters obtained from X-ray diffraction results.

Sample Code	a_o (Å)	$\beta_{(111)}$ (rad)	$D_{(111)}$ (nm)	T_C	$\varepsilon \times 10^{-4}$	$\delta \times 10^{-4}$ $(nm)^{-2}$
NiO-undoped	4.1730	0.231	37.1	1.4286	9.35512	7.2841
d_1	4.1724	0.191	44.8	1.1912	7.72954	4.97262
d_2	4.1720	**0.21**4	40.**1**	1.2140	8.65355	6.23256
d_3	4.1745	0.271	31.5	1.2171	11.00138	10.07331
d_4	4.1756	**0.20**3	42.**2**	1.1502	8.22502	5.63056
d_5	4.1731	0.199	43.**1**	1.2240	8.05402	5.39887

Academic Science Journal

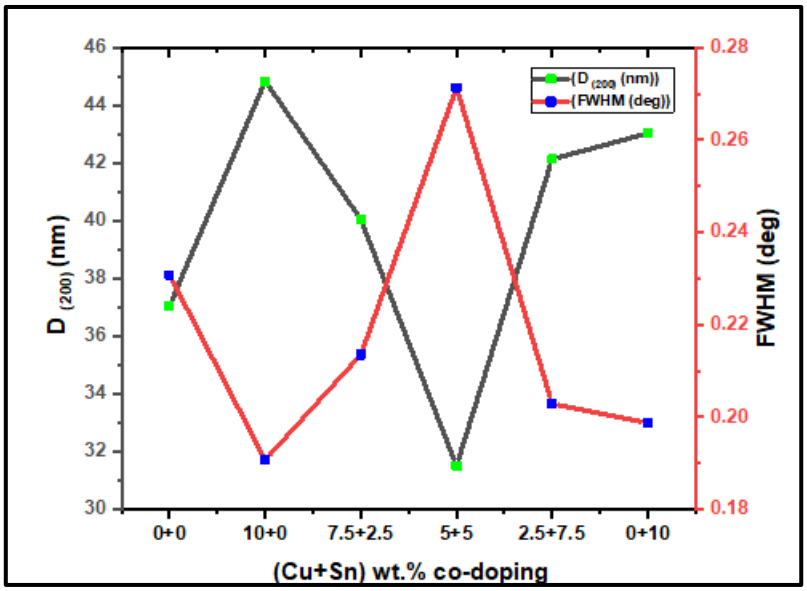

Figure 3: The relationship between (D_{200}) and (β_{200}) of undoped and doped NiO nanoparticles

Fourier Transform Infrared Spectroscopy (FTIR)

Infrared spectroscopy is used to detect the chemical bonds and functional groups associated with the compounds. Figure (4) shows the infrared spectrum of the prepared nanoparticles, as it is noted that there are broad absorption peaks due to the stretching vibration (Stretching Vibration). (O-H) of H_2O at the bounded region between (3200-3600 cm^{-1}) [12], as for the absorption peaks at the two regions (1566 and 1332 cm^{-1}) they go back to the bonds (H-O-H, C-H) respectively, the spectrum also showed absorption peaks in the region (400-500 cm^{-1}) which is due to the stretching vibration of the (Ni-O) band [13]. This confirms the improvement of the crystallization quality as previously mentioned in the properties of XRD because the occupation of Ions grafting to inter-sites leads to an increase in the grafting rate. The percentage of filled by grafting atoms (Cu + Sn) instead of oxygen atoms causes a decrease in the vibrational stretching patterns, which in turn leads to a decrease in the intensity of the peaks [14].

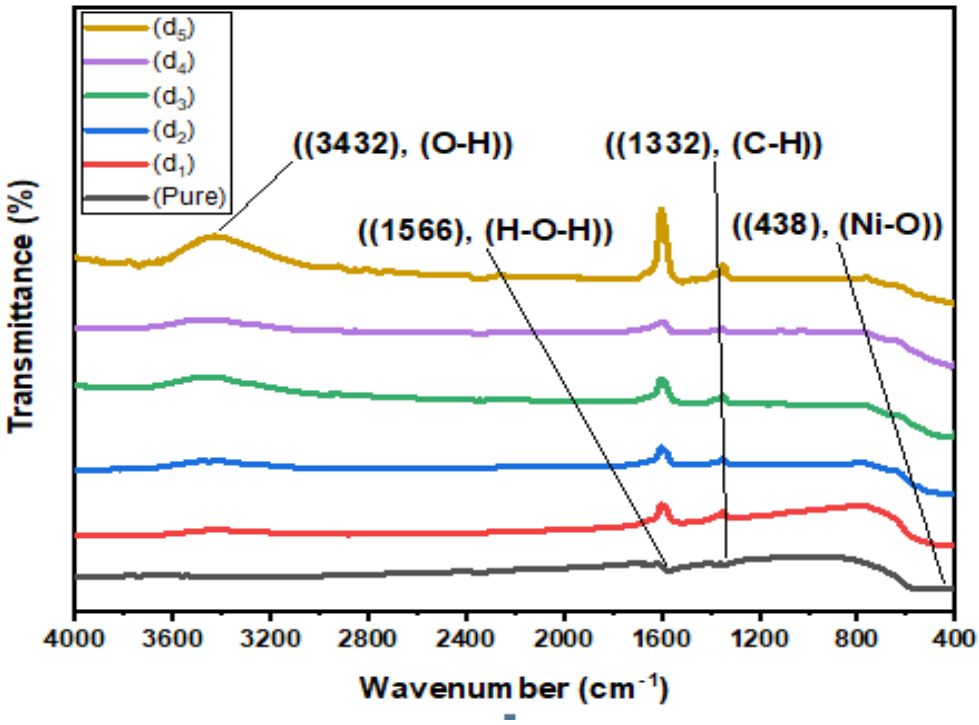

Figure 4: Infrared spectra of undoped and doped NiO nanoparticles.

Field Emission-Scanning Electron Microscopy (FE-SEM)

The growth and morphology of the surfaces of ungrafted nickel oxide (NiO) nanoparticles bi-doped with copper (Cu) and tin (Sn), prepared by the Sol-Gel method using the technology of the (FE-SEM) device with a very high capacity, was studied on each from zooming in and accurately imaging the surfaces of materials.

Figures (5) show images of different magnification powers (50 and 100 K_X) of undoped NiO grains doped with different [(Cu + Sn) co-Doping] nanoparticles. The images were analyzed using the Image J program for the purpose of calculating the average grain size and knowing the effect of doping on the composition of the nickel oxide granules, as shown in table (4). For undoping nickel oxide grains at annealing temperature (525 ^{o}C) and the largest value for particle size (40.358 nm) for NiO nanoparticles at [(2.5+7.5) (Cu + Sn) wt.%]. The pictures in Figure (5) show the growth and distribution of the grafted and ungrafted nickel oxide granules, as we

notice the good growth of the grafted (NiO) granules, and the granules take almost spherical or spherical shapes (Nano-spherical granules) and are well packed with different granular sizes, in addition to the formation of granular structures (Agglomeration of Grains), which take similar shapes. For the double-doped samples, it is noted that the effect of grafting seems clear to the grains, so that the different shapes of them resemble rock stones and others are spherical or semi-spherical (Rock Stones and Spherical or Semispherical Granules) with the appearance of agglomerations of nanoparticles in addition to voids and gaps clearly, with The clear difference is the appearance of better packed shapes and the disappearance and appearance of grain boundaries with different doping rates accompanied by an increase or decrease in the size of the grains due to the decrease or increase in the values of the microstrain as a result of the contribution of the copper and tin double doping atoms in the composition of NiO. The results of the FE-SEM examination obtained were almost in agreement with those obtained by the researchers.

Table 4: Values of average grain size of o undoped and doped NiO nanoparticles.

Sample Code	Grain Size (nm)
NiO-undoped	38.9
d_1	34.9
d_2	55.6
d_3	77.8
d_4	81.2
d_5	72.8

Academic Science Journal

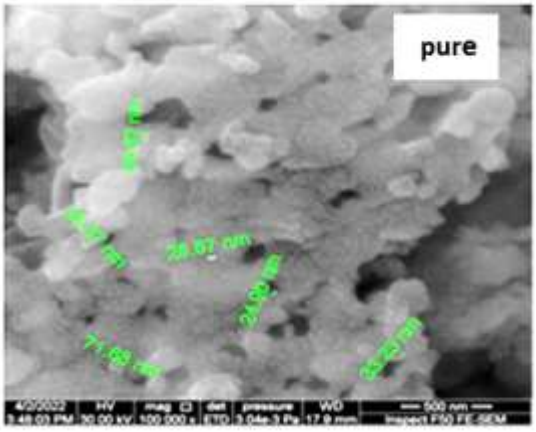

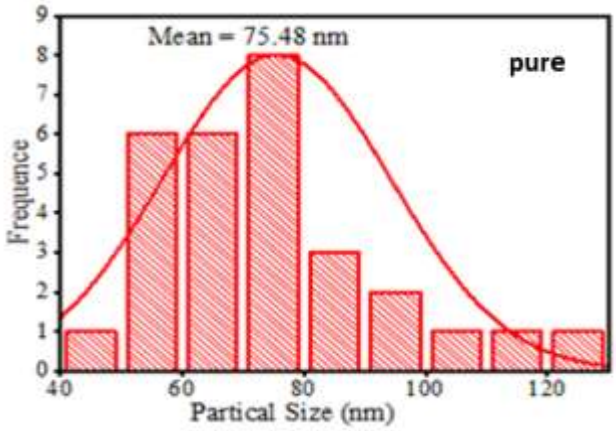

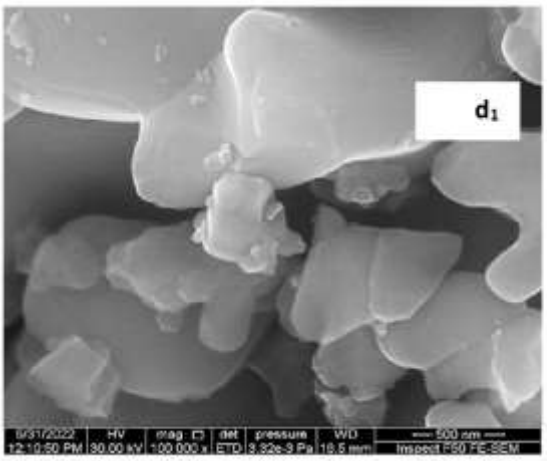

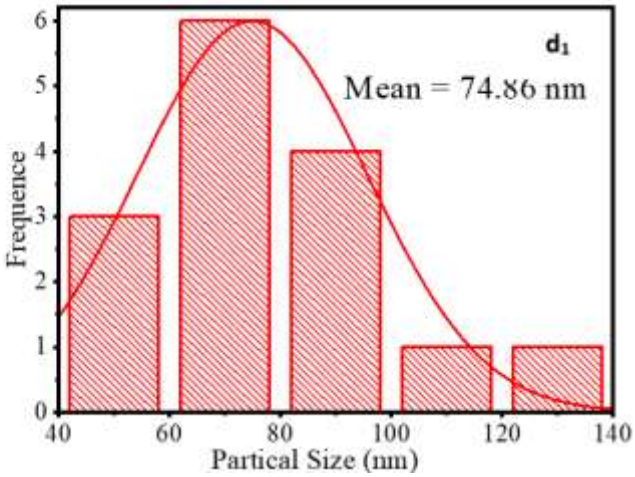

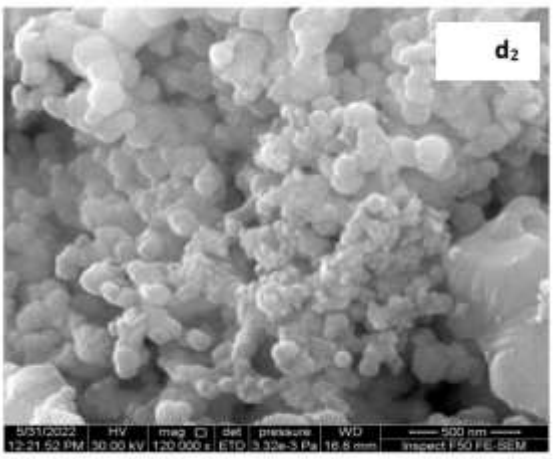

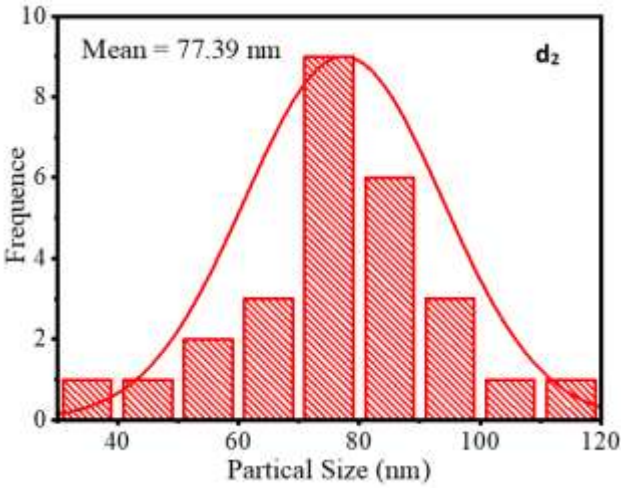

Academic Science Journal

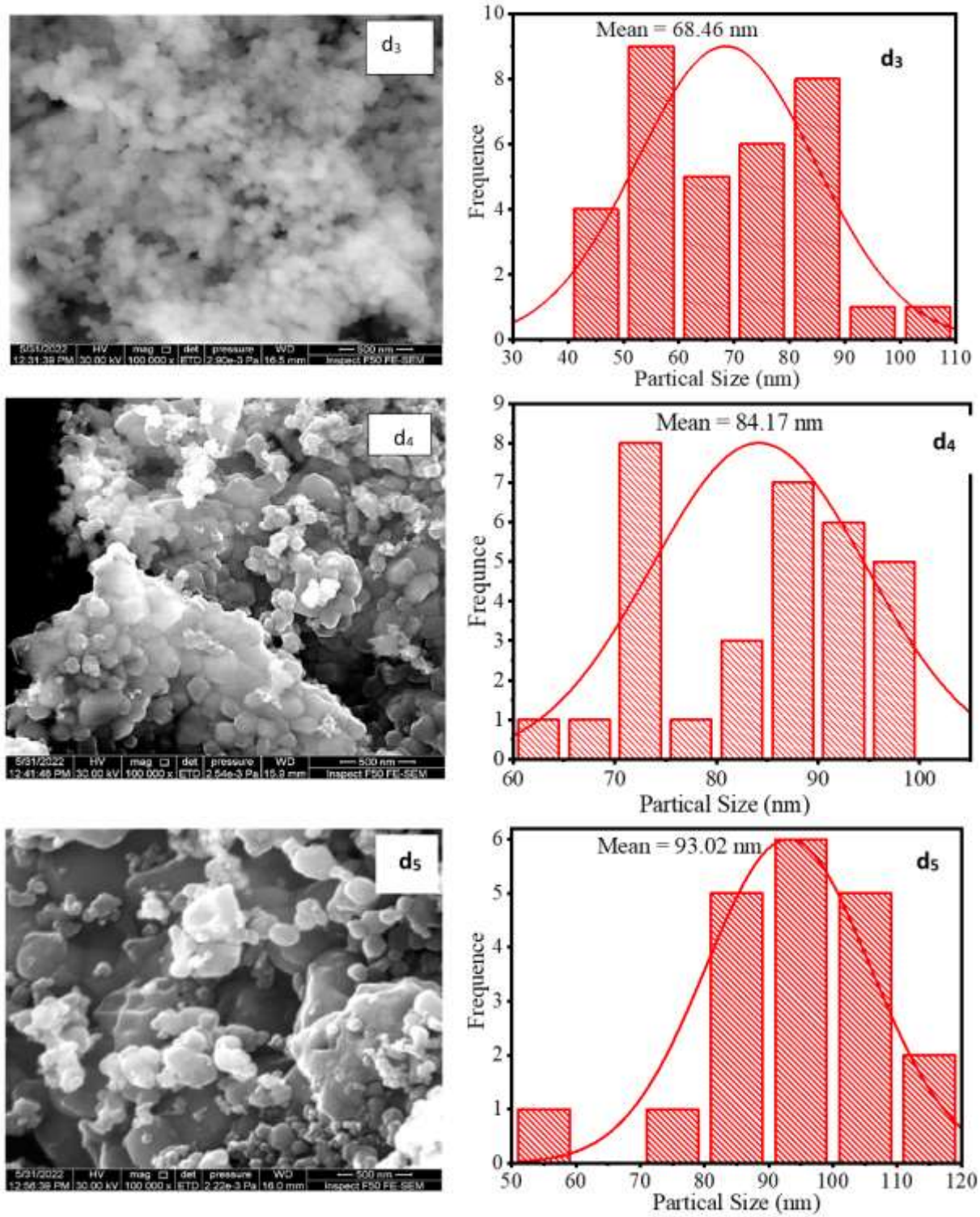

Figure 5: FE-SEM images of undoped and co-doped NiO nanoparticles

Academic Science Journal

Energy Dispersive Spectroscopy (EDS)

To assess the composition of undoped and co-doped NiO nanoparticles nickel oxide components, the examination was carried out using energy dispersal spectrometry (EDS). Figure (6) shows that the constituent elements of the granules are present, and that the quality of those elements is represented in the form of ratios of (Ni, Cu, Sn, O). As a result, the grafting process' success was verified, and the materials' proportions seemed to match what was done. It is applied to the process of making granules.

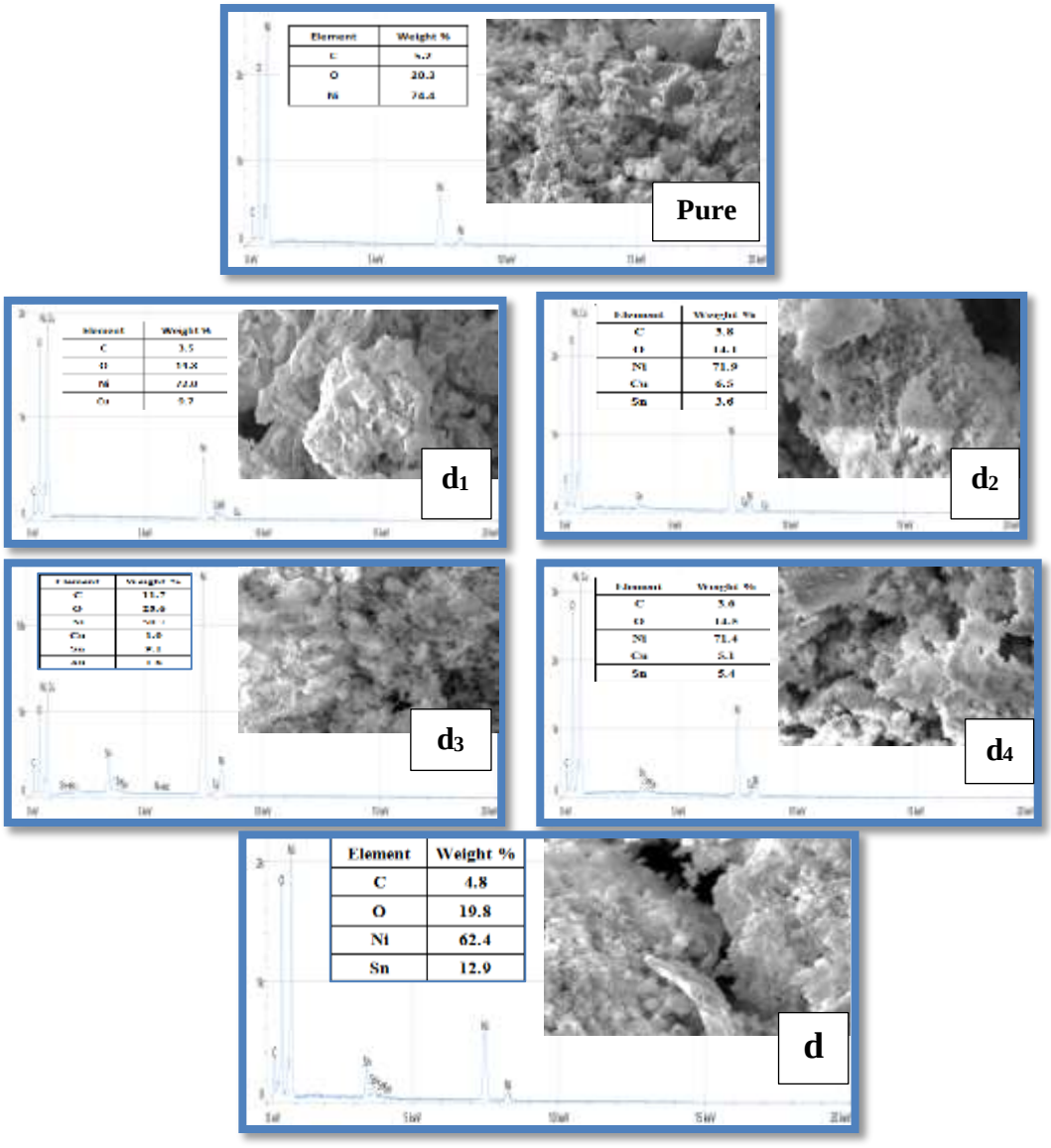

Figure 6: EDS analyzes of of undoped and co-doped NiO nanoparticles.

Optical Measurements

Absorbance (A)

Figure (7) shows the change in the absorbance spectrum for the undoped nickel oxide (NiO) nanoparticles and doped with different ratios of copper and tin as a function of wavelength change (200-1100 nm), as the absorbance values decrease with increases of the wavelength for all samples, because the spectrum values. The optical absorbance is dependent on the type of material and its crystal structure, as well as the energy of the incident photons. This results in a decrease in the absorbance of the prepared material for light with an increase in the wavelength (the energy of the photon is inversely proportional to the wavelength). When the energy of the photons is less than the optical energy gap of the semiconductor material, it causes a decrease in the absorbance values with the increase of the wavelength [16]. After the dual grafting of NiO granules as shown in Figure (5), we notice from the absorption spectrum that the behavior of the absorption spectrum of the samples is similar to its behavior before grafting, except that there is a decrease in the absorbance values except for the graft ratio [(5 + 5), (Cu + Sn) w %] It records the highest absorbance, and the absorption edge shifts towards high energies (Blue Shift) due to the occupancy of copper ions (Cu ions) compensating sites within the composition (NiO: Sn), which caused the homogeneity of the composition and reduced defects, and thus the lack of light scattering from the surface of the grains [17], and that the increase in the absorbance values of the grafted samples compared to the non-grafted samples may be due to the contribution of tin ions (Sn ions) and their occupation of inter-sites in the composition of the NiO: Cu lattice, which leads to an increase in the values of crystal and grain size [18], FE-SEM images and XRD measurements support this.

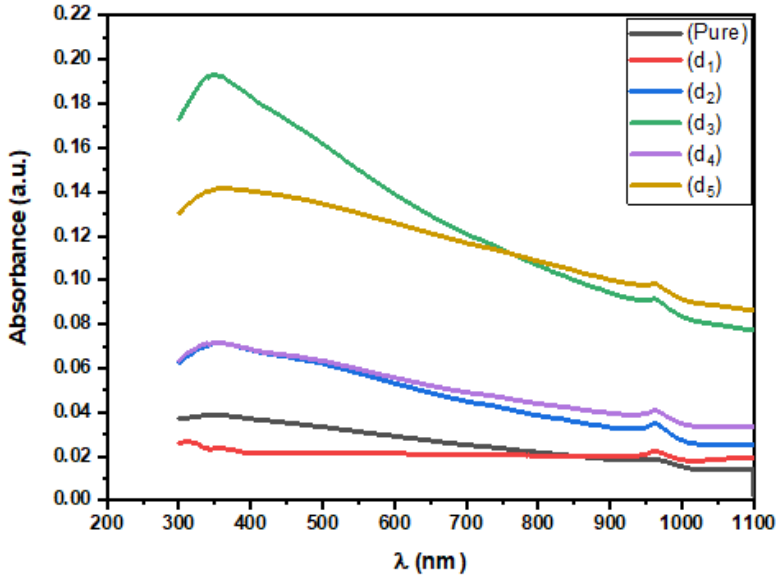

Figure 7: Absorbance spectrum of of undoped and doped NiO nanoparticles.

Transmittance (T)

The transmittance spectrum curve shown in Figures (8) shows an opposite behavior for the absorption spectrum of undoped nickel oxide (NiO) bi-doped with zinc and cobalt (Sn + Cu) within the wavelength range (200-1100 nm). Because the incident photons do not have enough energy to excite the electrons of the atoms of the prepared material, they are exhausted, and it is noted from the figure that the binary doping of NiO has led to a decrease in the transmittance and the reason for this is due to the entry of both copper ions and tin ions into interstitial sites within the structure of (NiO) or due to Increasing the scattering of light from the surface of the grains or due to oxygen deficiencies [119], while the binary grafted sample with the ratios [(0 + 10) (Cu + Sn) w.%] of the NiO grains caused an increase in the permeability in a way that makes it suitable as materials from which it is made Transparent windows for photovoltaic applications. The reason for the increase in transmittance, as mentioned earlier, is due to the decrease in local levels, according to the Burstein Moss displacement, as well as the improvement in the crystallization of the film (decreasing point defects) due to the contribution of copper ions (Cu ions) in the structure of the (NiO: Sn) lattice) [120].

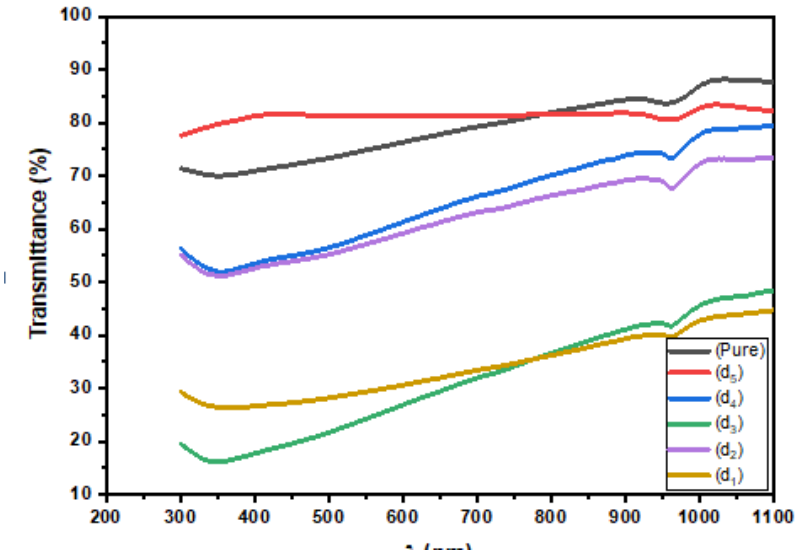

Figure 8: Transmittance spectrum of of undoped and co-doped NiO nanoparticles.

Absorption Coefficient (α)

The values of the absorption coefficient (α) for pure (NiO) granules were calculated through The values of the absorption coefficient (α) of undoped (NiO) particles bi-doped with copper (Cu) and tin (Sn) were calculated through the relationship (2-20), and Figure (9) shows the change of absorption coefficient for all the prepared solutions as a function of energy The incident photon, as it is clear that the behavior of the absorption coefficient curves is similar to the behavior of the absorption spectrum due to the nature of the relationship between them (2-20). Its value (α≥101-4 cm-1)) becomes near the basic absorption edge region, and then the values of the absorption coefficient continue to gradually increase for the ranges of incident photon energies that exceed the values of the optical energy gap (EPh>Eg) for all the prepared granules, and this indicates the possibility of (Allowed) direct electronic transitions between the valence and conduction bands at those energies, because high values of the absorption coefficient and greater than (104 cm-1) indicate the possibility of allowed direct electronic transitions [21]. It is noted from the figure that the behavior of the absorption coefficient curves changes with the change in the grafting rates, some of them behave the same as the ungrafted granules with an increase in its value at the ratio (5 + 5 w%) due to the increase in the absorbance of the granules as a result of grafting, which caused the filling of the oxygen spaces

with the graft ions (Cu ions) and (Sn ions) as mentioned previously, and thus a decrease in the optical energy gap values, and it was also found that the values of the absorption coefficient decrease with some ratios of binary grafting, and the creep of the absorption edge towards high photon energies, which leads to an increase in the values of the optical energy gap, and the reason for this is as We have already mentioned that the zinc (Cu) atoms occupy compensatory or substitutional sites in the NiO:Sn lattice.

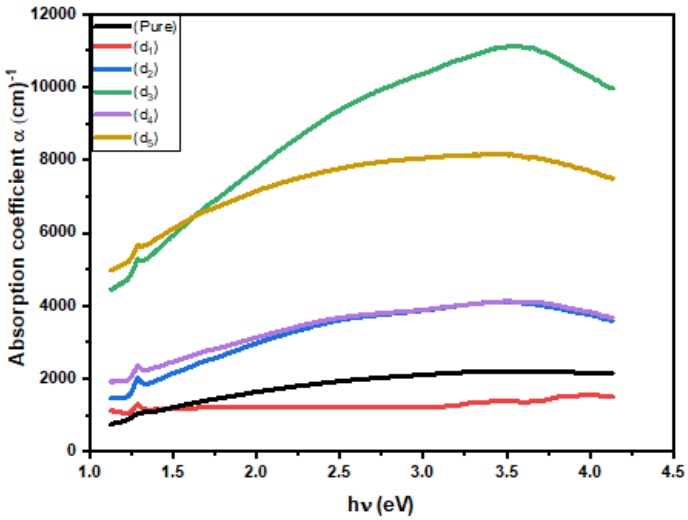

Figure 9: Absorption coefficient (α) for undoped and co-doped NiO nanoparticles.

Photoluminescence Measurement

Figure (10) shows the photoluminescence measurement of nickel oxide nanoparticles before and after doping and annealed at a temperature (525 ºC), as shown in Figure (10). The sample before doping has a peak value of (489.3 nm), this is identical approx to the results of the absorption spectrum of the nickel oxide nanoparticles. We note from the same figure that the double-grafted grains record peak values at (368.1, 681.1, 582.2, 772.7, 438.6 nm) for (d_1, d_2, d_3, d_4 and d_5) respectively, and this is almost identical to the results of the absorption spectrum of the prepared nanoparticles. The results show that the sample (d_1) recorded the highest value of photoluminescence compared to the other samples. Table (5) shows the values of the energy gap of undoped and doped NiO nanoparticles.

Academic Science Journal

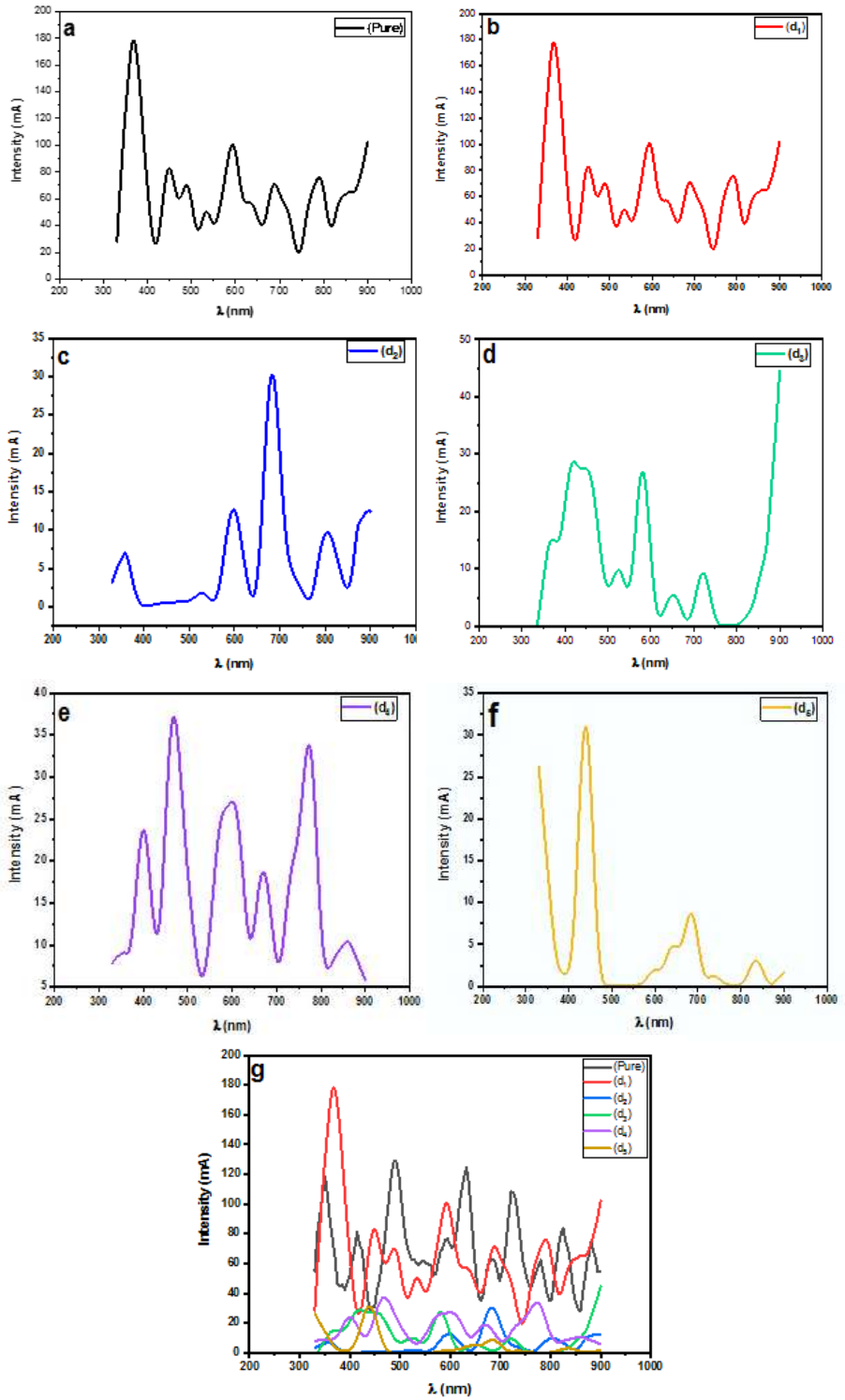

Figure 10: Photoluminescence measurement of for undoped and co-doped NiO nanoparticles.

Table 5: Values of energy gap of undoped and doped NiO nanoparticles.

Sample Code	Eg (eve)
NiO-undoped	3.377
d_1	3.369
d_2	1.821
d_3	2.129
d_4	1.704
d_5	2.827

Conclusions

In this work, Sol-Gel method was used to prepare undoped and doped NiO nanoparticles with Cu and tin. Scherrer's equation was used to calculate the crystallite size of the samples, and it was discovered that the crystallite size (7.2841, 4.97262, 4.97262, 10.07331, 5.63056 and 5.39887 nm) for NiO- pure, d_1, d_2, d_3, d_4 and d_5 respectively. The image of FESEM exhibited a spherical nanoparticle structure for NiO. The presence of a strong band at 425 cm-1 in nanoparticles indicates the spinal structures of Ni–O of FTIR analysis. The band gap values increase with increased molar ratios. FTIR spectrum of NiO NPs, showed absorption peaks at the two regions (1566 and 1332 cm^{-1}) they go back to the bonds (H-O-H, C-H) respectively, the spectrum also showed absorption peaks in the region (400-500 cm-1) which is due to the stretching vibration of the (Ni-O) band. The energy gap changes between increases and decreases with the change in doping rate.

References

1. H. Abbas, K. Nadeem, A. Hafeez, A. Hassan, N. Saeed, H. Krenn, Ceramics International, 45(14), 17289-17297(2019)
2. Y. Huang, Y. Zhang, S. Lin, L. Yan, R. Cao, R.Yang, W. Xiang, Journal of Alloys and Compounds, 686, 564-570(2016)
3. S. Wang, S. P. Jiang, X. Wang, Electrochim, Acta, 56, 3338–3344(2011)

4. N. A. Bakr, S. A. Salman, A. M. Shano , International Journal of Current Research, 6(11), 9644-9652(2014)
5. Z. T. Khodair, A. A. Kamil, Y. K. Abdalaah, Physica, B503,55–63, (2016)
6. M. Thirumoorthi, J. T. J. Prakash, J. Asian Ceram. Soc., 4(1), 39–45(2016)
7. T. Noorunnisha, Appl. Phys. A Mater. Sci. Process., 126(10), 1–9(2020)
8. G. Turgut, J. Mater. Sci. Mater. Electron., 28(22), 16992–17001(2017)
9. M. Anitha, K. Saravanakumar, N. Anitha, L. Amalraj, Appl. Surf. Sci., 443, 55–67(2018)
10. B. Varshney, M. J. Siddiqui, A. H. Anwer, M. Z. Khan, F. Ahmed, A. Aljaafari, H. H. Hammud, A. Azam, Scientific Reports, 10(1), (2020)
11. S. W. Shin, G. L. Agawane, ,I. Y. Kim, S. H. Jo, M.S. Kim, G. S. Heo, J. H. Kim, J. Y. Lee, Surf. Coatings Technol., 231, 364–369(2013)
12. Y. Thaver, S. O. Oseni, G. T. Mola, Solar Energy, 214, 11–18(2021)
13. A. Yazdani, H. Zafarkish, K. Rahimi, Materials Science in Semiconductor Processing, 74, 225–231(2018)
14. K. Nadeem, A. Ullah, M. Mushtaq, M. Kamran, S. S. Hussain, M. Mumtaz, Journal of Magnetism and Magnetic Materials, 417, 6–10(2016)
15. N. M. Hosny, Polyhedron, 30(3), 470–476(2011)
16. Bi-doped CdO thin films by sol–gel spin coating method" Mater. Lett., vol. 80, 127–130(2012)
17. D. Mateos, B. Valdez, J. R. Castillo, N. Nedev, M. Curiel, O. Perez, A. Arias, H. Tiznado, Ceramics International, 45(9), 11403–11407(2019)
18. A. A. Sery, W. A. A. Mohamed, F. F. Hammad, M. M. H. Khalil, H. K. Farag, Materials Chemistry and Physics, 275, 125190(2022)
19. V. A. Pandey, S. Munjal, T. Ahmad, Structural and optical properties of sol gel synthesized NiO nanoparticles, In: AIP Conference Proceedings, 2270(1), 110011). AIP Publishing LLC., (2020)
20. M. P. Deshpande, K. N. Patel, V. P. Gujarati, K. Patel, S. H. Chaki, Advanced Materials Research, 1141, (2016)
21. J. Tasbandi, A. Koushki, H. Eshghi, Optical and Quantum Electronics, 49(3), (2017)